

Research Article

# Characterization of cellular senescence in radiation ulcers and therapeutic effects of mesenchymal stem cell-derived conditioned medium

Wanchao Chen<sup>1,†</sup>, Yang Wang<sup>1,†</sup>, Jiancheng Zheng<sup>1</sup>, Yan Chen<sup>1</sup>, Can Zhang<sup>1</sup>, Wei Yang<sup>1</sup>, Lingling Wu<sup>1</sup>, Zeyu Yang<sup>2</sup>, Yu Wang<sup>1</sup> and Chunmeng Shi<sup>1,\*</sup>

<sup>1</sup>Institute of Rocket Force Medicine, State Key Laboratory of Trauma, Burns and Combined Injury, Third Military Medical University (Army Medical University), 400038, Chongqing, China and <sup>2</sup>Breast and Thyroid Surgical Department, Chongqing General Hospital, 401147, Chongqing, China

\*Correspondence. Email: shicm@sina.com

†These authors contributed equally to this work.

Received 21 October 2022; Revised 16 November 2022; Editorial decision 11 January 2023

## Abstract

**Background:** Radiation ulcers are a common and severe injury after uncontrolled exposure to ionizing radiation. The most important feature of radiation ulcers is progressive ulceration, which results in the expansion of radiation injury to the nonirradiated area and refractory wounds. Current theories cannot explain the progression of radiation ulcers. Cellular senescence refers to as irreversible growth arrest that occurs after exposure to stress, which contributes to tissue dysfunction by inducing paracrine senescence, stem cell dysfunction and chronic inflammation. However, it is not yet clear how cellular senescence facilitates the continuous progression of radiation ulcers. Here, we aim to investigate the role of cellular senescence in promoting progressive radiation ulcers and indicate a potential therapeutic strategy for radiation ulcers.

**Methods:** Radiation ulcer animal models were established by local exposure to 40 Gy X-ray radiation and continuously evaluated for >260 days. The roles of cellular senescence in the progression of radiation ulcers were assessed using pathological analysis, molecular detection and RNA sequencing. Then, the therapeutic effects of conditioned medium from human umbilical cord mesenchymal stem cells (uMSC-CM) were investigated in radiation ulcer models.

**Results:** Radiation ulcer animal models with features of clinical patients were established to investigate the primary mechanisms responsible for the progression of radiation ulcers. We have characterized cellular senescence as being closely associated with the progression of radiation ulcers and found that exogenous transplantation of senescent cells significantly aggravated them. Mechanistic studies and RNA sequencing suggested that radiation-induced senescent cell secretions were responsible for facilitating paracrine senescence and promoting the progression of radiation ulcers. Finally, we found that uMSC-CM was effective in mitigating the progression of radiation ulcers by inhibiting cellular senescence.

**Conclusions:** Our findings not only characterize the roles of cellular senescence in the progression of radiation ulcers but also indicate the therapeutic potential of senescent cells in their treatment.

**Key words:** Ionizing radiation, Radiation ulcer, Cellular senescence, uMSC-CM

---

## Highlights

- Radiation ulcer animal models with features of clinical patients were established to investigate the mechanism of progressive radiation ulcers.
  - Cellular senescence is characterized by the continuous progression of radiation ulcers.
  - Senescent cell secretions facilitate paracrine senescence and promote the progression of radiation ulcers.
  - uMSC-CM is effective in mitigating the progression of radiation ulcers by inhibiting cellular senescence.
- 

## Background

Radiation-induced skin injury caused by uncontrolled exposure to ionizing radiation has recently become common because of the rapid increase in the use of radiation technology in different fields of industry and medicine. Approximately 95% of cancer patients who receive radiotherapy will develop radiation-induced dermatitis of varying severity [1] and fluoroscopy-guided interventional procedures have also been recognized as an important risk for radiation-induced skin injury [2]. Radiation-induced skin injury is typically characterized by erythema, hyperpigmentation, edema and dry or moist desquamation. More importantly, high-dose or multiple irradiations can induce more severe radiation ulcers, which are the most distressed skin injuries and seriously impact quality of life [3]. Radiation ulcers often last for several months to years and are accompanied by prolonged inflammation, delayed wound healing and progressive ulceration. Among them, the continuous progression of ulceration can induce radiation ulcers to expand from the irradiated skin to the nonirradiated area and even erode vital organs or cause fatal reactions, which is considered a critical difficulty in the treatment of radiation ulcers [4]. Although necrosis and chronic inflammation were found to be important mechanisms involved in radiation ulcers in previous studies, the primary pathological mechanism responsible for the continuous progression of radiation ulcers remains unclear. Meanwhile, current interventions, such as corticosteroids, growth factors and engineered wound dressing, cannot effectively mitigate the progression of radiation ulcers [5]. Thus, further research efforts are urgently needed to uncover the primary mechanisms responsible for the progression of radiation ulcers and novel therapeutic strategies are required to manage and prevent the risk of continuous progression in radiation ulcers.

Ionizing radiation directly induces DNA damage and reactive oxygen species (ROS) production has long been believed to be the main cause of radiation-induced injury [6,7]. However, radiation-induced cell death and oxidative stress injury cannot fully explain the pathological characteristics of radiation ulcers with persistent tissue damage and continuous

progression of ulceration. In addition, it is well known that ionizing irradiation is also an important cause of cellular senescence [8,9]. Radiation contributes to increased ROS production and persistent DNA damage, which activates the p53/p21<sup>CIP1</sup> and p16<sup>INK4a</sup>/Rb regulatory pathways and results in cell cycle arrest inducing cellular senescence [10,11]. Many studies have indicated that senescent cells exist extensively in different types of chronic wounds, which directly or indirectly affect various processes of wound healing and tissue regeneration through a variety of mechanisms [12]. Previous studies have reported that pharmaceutical inhibition of cellular senescence via NRF2 and AMPK could prevent radiation ulcers [13]. However, the characteristics of cellular senescence in the progression of radiation ulcers and the underlying roles of senescent cells in promoting radiation ulcer progression remain to be further clarified. At the same time, more convincing evidence that senescent cells can serve as practical therapeutic targets for radiation ulcer treatment is also needed.

In this study, radiation ulcer animal models were established by exposing the local skin of rats to X-ray irradiation, and the characteristics of cellular senescence and the functions of senescent cells in the continuous progression of radiation ulcers were studied. Our results indicated that senescent cells increased as radiation ulcers progressed, and different senescent cell types appeared in different proportions during the continuous progression of radiation ulcers. In particular, exogenous injection of senescent cells was proven to significantly promote radiation ulcer progression in rat models, indicating the pivotal role of senescent cells in the progression of radiation ulcers. A mechanistic study indicated that specific senescent cell secretions might play important roles in contributing to cellular senescence in radiation ulcers and promoting chronic radiation ulcer progression. Moreover, conditioned medium from human umbilical cord mesenchymal stem cells (uMSC-CM) was used to treat radiation ulcers in animal models, and our results indicated that uMSC-CM significantly mitigated the progression of radiation ulcers by inhibiting cellular senescence. The results have further demonstrated the critical roles of senescent cells in the

progression of radiation ulcers and suggest that senescent cells could serve as a practically effective target for radiation ulcer therapy. Thus, our studies have provided new insights into the pivotal roles of cellular senescence in the pathological mechanisms and progression of radiation ulcers and suggested a potential strategy for the treatment of radiation ulcers targeting cellular senescence.

## Methods

### Establishment of radiation ulcer animal models

The animal studies were in accordance with the Animal Care and Use Committee of the Army Medical University. Male Sprague–Dawley (SD) rats (6–8 weeks) purchased from the Laboratory Animal Center of the Army Medical University were used to establish radiation ulcer models. Rat limb skin radiation ulcer models were established as previously described [14]. In brief, 10% chloral hydrate sodium was used for rat anesthesia, and rats' left posterior limbs were exposed to radiation for 45 min with a total dose of 40 Gy (Precision X-ray; filter: 2 mm Al; 0.9 Gy/min) and other body parts were shielded with lead plates. Then, irradiated rats were randomly divided into eight groups ( $n = 5$ ) and examined at different times (0, 8, 16, 20, 30, 60, 120 and 260 days) after irradiation.

For the radiation ulcer models of back skin, rats were anesthetized and a 2.2×1.8 cm full-thickness skin U-shaped incision was made in the middle of the rat back. Then, the skin was turned up and attached to the lead plate, other parts of the rat body were blocked with a lead plate and the U-shaped skin was given a single dose of 40 Gy irradiation as previously described. The skin was then sutured back to its original site after irradiation.

### Score evaluation

Radiation-induced skin injury was examined by two blinded observers after irradiation of the local skin of rats. The degree of skin damage was scored as shown in Table S1 (see online supplementary material) according to previous skin score criteria for an animal model [15]. Skin damage was measured every 2 days, once a week after 60 days, and continuously for 38 weeks.

### Tissue staining and pathological examination

Rat skins were taken at each time point and fixed in 4% paraformaldehyde for >24 h, paraffin-embedded and sliced into sections of 3  $\mu\text{m}$ , and the sections were stained with hematoxylin and eosin (H&E) to examine histopathological changes. Masson trichrome staining (Nanjing Jiancheng, D026–1-2) was used to detect skin fibrosis according to the manufacturer's protocols. An In Situ Cell Death Detection Kit (Roche, 11684817910) was used for the terminal deoxynucleotidyl transferase-mediated fluorescein-dUTP nick-end labeling

(TUNEL) staining assay to analyze cell apoptosis after irradiation. The experiment was repeated on three different specimens for each group.

### Immunofluorescence

The paraffin-embedded skin sections were deparaffinized and rehydrated. After antigen retrieval with citrate buffer the slides were incubated with goat serum blocking solution for 40 min at room temperature and then with primary antibodies against p16 (Abcam, ab54210), p21 (Santa Cruz, sc817), Ki67 (Abcam, ab15580), phosphorylated histone H2AX ( $\gamma$ -H2AX; Abcam, ab81299), platelet endothelial cell adhesion molecule-1 (CD31; Abcam, ab182981),  $\alpha$ -smooth muscle actin ( $\alpha$ -SMA; Abcam, ab32575) and mouse EGF-like module-containing mucin-like hormone receptor-like 1 (F4/80; Proteintech, 28463–1-AP). For cultured cell staining, cells were fixed in 4% paraformaldehyde and blocked with goat serum for 1 h. Then, the cells were permeabilized with 0.25% Triton X-100 for 10 min and incubated with the primary antibody at 4°C overnight, nuclei were stained with 4',6-diamidino-2-phenylindole and cells were observed using a fluorescence microscope (Thermo, ES500).

### Senescence-associated $\beta$ -galactosidase staining

For cell staining, the cultured cells were seeded into 6-well plates and fixed in 2 ml of 4% paraformaldehyde. Then, the cells were stained with the staining solution (Beyotime, C0602, pH=6.0, China) at 37°C for 24 h. For skin tissue staining, 6  $\mu\text{m}$  frozen sections of tissues were fixed with 4% paraformaldehyde and washed with PBS, then incubated in senescence-associated  $\beta$ -galactosidase (SA- $\beta$ -Gal) staining solution as described above. The senescent cells were identified as blue-stained cells under light microscopy.

### Primary cell isolation and senescent fibroblast establishment

Primary dermal fibroblasts were isolated from dermal tissues in neonatal SD rats as previously reported [13]. In brief, skin tissues were cut into 1–2 mm pieces and digested for 1 h at 37°C in digestion medium containing 8 mg/ml collagenase III (Diamond, A004180–0100) and then digested with trypsin at 37°C for 30 min. Then, the cells were filtered through a 75  $\mu\text{m}$  cell strainer and cultured in DMEM medium supplemented with 10% fetal bovine serum and 1% streptomycin/penicillin.

To induce senescent fibroblasts, primary dermal fibroblasts were isolated from dermal tissues in neonatal SD rats as previously described. After fibroblasts were isolated and attached to the wall, the cells were exposed to radiation for 9 min with a total dose of 8 Gy (Precision X-ray; filter: 2 mm Al; 0.9 Gy/min). Then, the irradiated fibroblasts were cultured normally for 7 days and the senescent phenotypes of the fibroblasts were identified by SA- $\beta$ -gal staining and immunofluorescence staining.

### Conditioned medium

The conditioned medium (CM) from senescent cells was collected from radiation-induced senescent cells after culture in fresh medium for 24 h. uMSC-CM was prepared as previously reported [16]. Fourth passage uMSCs were incubated in serum-free  $\alpha$ -MEM culture medium for 12 h and the conditioned medium was collected and concentrated in the chromatography cabinet using an ultrafiltration membrane with a molecular weight of 5000 daltons at 4°C and then filtered with a 0.22  $\mu$ m membrane to remove bacteria. Then, uMSC-CM lyophilized powder was obtained by freezing at -90°C for 4 h.

### RNA-sequencing analysis

The irradiation-induced primary senescent cells and the CM-induced secondary senescent cells were identified by SA- $\beta$ -gal staining and immunofluorescence staining, and then cells were collected for RNA sequencing. Total RNA from each sample was extracted by TRIzol (Invitrogen, Carlsbad, CA, USA) reagent. Then, the RNA was qualified and quantified using a NanoDrop and Agilent 2100 bioanalyzer, respectively (Thermo Fisher Scientific, MA, USA). RNA libraries were created using the NEBNext<sup>®</sup> Ultra<sup>™</sup> Directional RNA Library Preparation Kit from Illumina<sup>®</sup> (Illumina, San Diego, CA). The libraries were then sequenced by a commercial sequencing company using the Illumina NovaSeq<sup>™</sup> 6000 platform.

The sequencing data were filtered using SOAPnuke (v1.5.2). The clean reads were mapped to the reference genome using HISAT2 (v2.0.4). Bowtie2 (v2.2.5) was applied to align the clean reads to the reference coding gene set and then the expression level of the gene was calculated by StringTie (v2.1.2) [17]. The heatmap was drawn by pheatmap (v1.0.8). In addition, differential expression analysis was performed using DESeq2 (v1.4.5) with a  $Q$  value  $\leq 0.05$ . The GO (<http://www.geneontology.org/>) and Kyoto Encyclopedia of Genes and Genomes (KEGG) (<https://www.kegg.jp/>) enrichment analyses of annotated differentially expressed genes (DEGs) were performed by Phyper (<https://en.wikipedia.org/wiki/>) hypergeometric distribution using the hypergeometric test. The significance levels of terms and pathways were corrected by the  $Q$  value with a rigorous threshold ( $Q$  value  $\leq 0.05$ ) by the Bonferroni correction method.

### Western blotting

Total proteins from samples were extracted using RIPA buffer containing a protease inhibitor cocktail (Roche, 5 892 791 001). The protein concentrations were determined using a BCA kit (Beyotime, P0010s). After electrophoresis, proteins were transferred to PVDF membranes (Millipore, E1078). PVDF membranes were blocked and incubated with corresponding primary antibodies, including p16 (Santa Cruz, sc1161), p21 (Santa Cruz, sc817), p53 (Santa Cruz, sc126), nuclear lamina protein LMNB1 (lamin B1; Beyotime,

AF-1408) and  $\beta$ -actin (Zen Bio, 700 068), at 4°C overnight, followed by incubation with secondary antibodies for 1 h at room temperature. Enhanced chemiluminescence detection was performed after the membrane was washed.

### Enzyme-linked immunosorbent assay

According to the manufacturer's protocol, the concentrations of the rat inflammatory cytokines interleukin-1 $\alpha$  (IL-1 $\alpha$ ) and angiopoietin-1 (ANG-1) in plasma samples were measured with IL-1 $\alpha$  (CUSABIO, CSB-E04622r) and ANG-1 (CUSABIO, CSB-E07303r) enzyme-linked immunosorbent assay (ELISA) kits, respectively.

### Statistical analysis

All data in the study are presented as the means  $\pm$  standard deviations. Statistical analyses were applied using one-way and two-way analyses of variance (ANOVA) with Bonferroni's *post hoc* comparison. Statistical significance is denoted by an asterisk ( $*p < 0.05$ ;  $**p < 0.01$ ). Statistical analyses were carried out using GraphPad Prism 9.0 (GraphPad Software Inc., San Diego, CA, USA).

## Results

### Establishment and characterization of radiation ulcers in rat models

To further characterize the pathologic mechanism and progression of radiation ulcers, radiation ulcer animal models were established by exposure of rat posterior limbs to X-ray radiation at a single dose of 40 Gy (Precision X-ray; filter: 2 mm Al; 0.9 Gy/min) and skin injury was evaluated continuously for >260 days. As shown in Figure 1a, visible skin damage was detected at 8 days after irradiation with superficial skin tissue edema. At day 16, the skins of irradiated rats showed a typical ulcer phenotype with erythema, large areas of hair loss and the adhesion of toes. However, the erythema of the injured skin was decreased with relief of ulceration phenotypes at day 20. At day 30, all of the radiation-induced injured skin was replaced by scar tissue, showing signs of remission with a dry and clean appearance in the irradiated limbs. However, we found that the irradiated skins again showed an aggravated phenotype with repeated ulceration and scabbing beginning on day 45. Then, the skin ulcers continued to progress, and the irradiated limbs showed hardening, desquamation and contracture to the proximal end. In the late stage of radiation injury (120–260 days), the skin ulcers were enlarged from the irradiated area to the nonirradiated area. Skin injury was scored according to the previous skin damage scoring standard [15] (Table S1) to further analyze the progressive characteristics of ulcer radiation. We found that the skin damage score gradually increased with the progression of radiation ulcers but was accompanied by a slight decrease 20–30 days after irradiation (Figure 1b). This result was consistent with the gross observation of radiation ulcer models and suggested

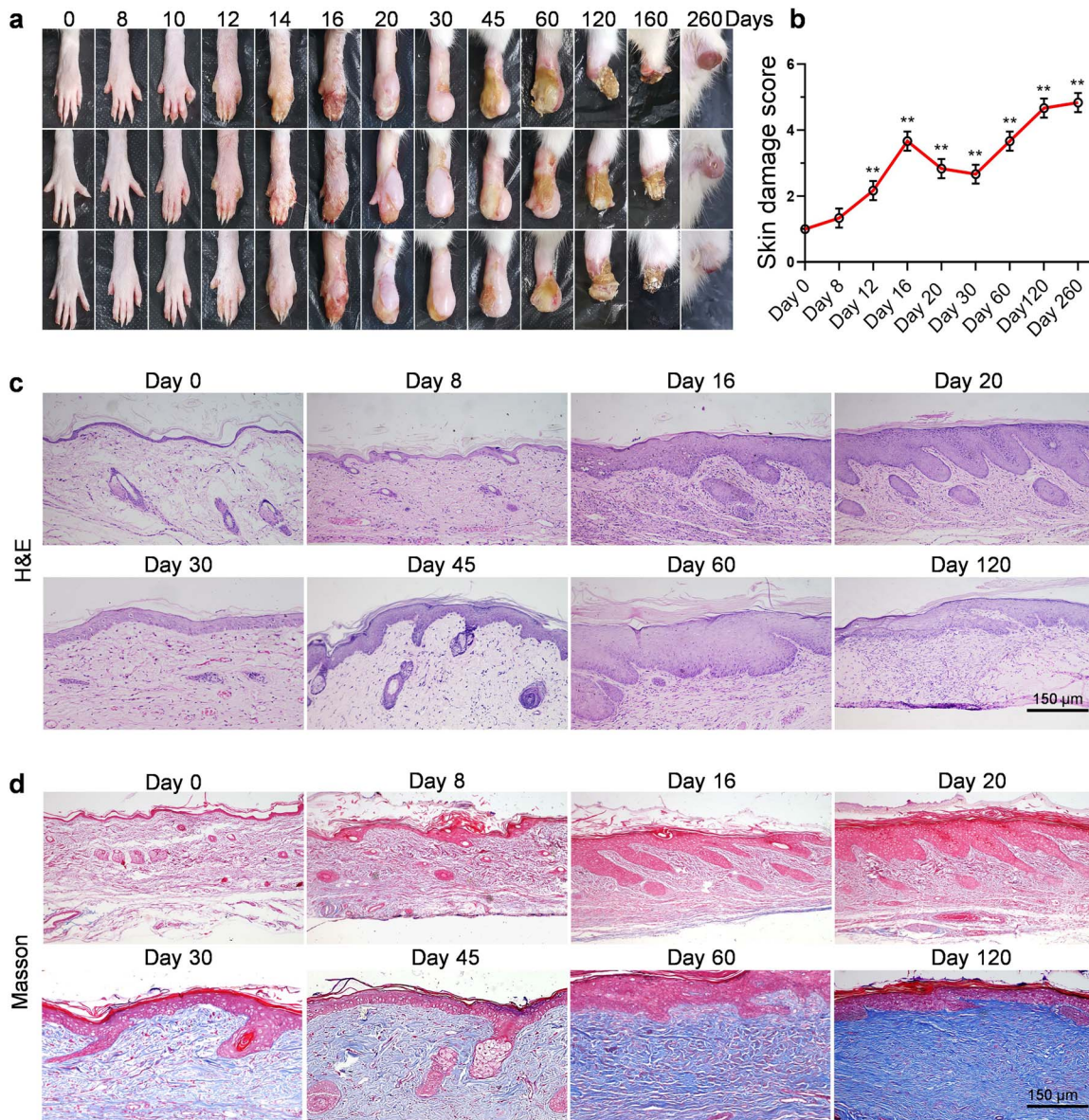


**Figure 1.** Characterization and histopathological analysis of radiation ulcer models. (a) Representative images of limbs from irradiated rats at different times (40 Gy of irradiation). (b) Skin injury was scored according to skin damage scoring standards. (c) Histological analysis of rat skin tissues in radiation ulcer models. (d) Masson staining analysis of rat skin tissues in radiation ulcer models. Data are presented as mean  $\pm$  standard deviation,  $n=3$ , one-way analysis of variance with Bonferroni's *post hoc* comparison, compared with day 0; \*\* $p < 0.01$ . H&E hematoxylin and eosin staining

transient symptomatic relief during the progression of radiation ulcers. Furthermore, H&E staining of skin tissue was performed to detect histopathological changes in irradiated skin and showed that the thickness of the epidermis was increased after radiation, infilling with a large number of inflammatory cells in the epidermis and dermis. Similarly, epidermal thickening and inflammatory cell infiltration were decreased at day 30 after irradiation, indicating symptomatic alleviation. Then, the radiation ulcer continued to progress, and the thickness of the epidermis increased again with a significant decrease in skin appendages, such as hair follicles, on day 60. On the 120th day, the necrosis and contraction of irradiated skin was obvious, resulting in a thin skin layer (Figure 1c). Masson's trichrome staining showed that the

degree of skin fibrosis gradually increased after irradiation (Figure 1d). Thus, these results indicated that the established radiation ulcer animal models mimicked the progression of radiation ulcers in patients and could be extrapolated to investigate the pathological mechanisms of radiation ulcers. Radiation-induced DNA damage and oxidative stress are the main causes of radiation injury. Immunofluorescence detection of  $\gamma$ -H2AX, a marker of the DNA damage response, indicated the persistence of DNA damage in skin after irradiation (Figure 2a, b). The TUNEL assay showed an increased number of apoptotic cells in irradiated skin tissues (Figure 2c, d). Immunofluorescence showed a significant decrease in cell proliferation in irradiated skin tissues with a reduction in Ki67 cells (Figure 2e, f). In conclusion, all these results

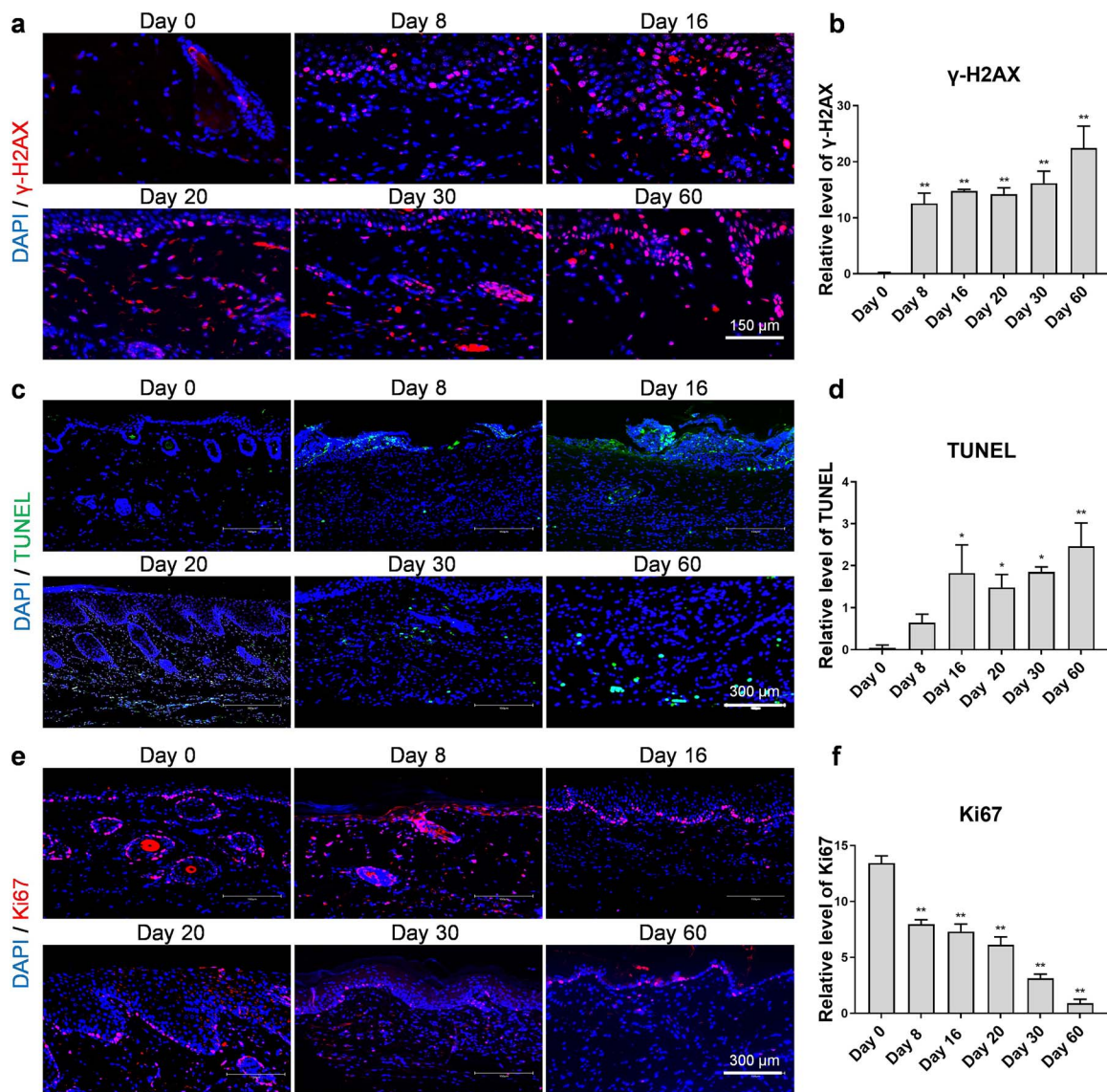


**Figure 2.** Continuous analysis of DNA damage and cell functional changes in radiation ulcer models. (a, b) Representative immunofluorescence pictures of  $\gamma$ -H2AX in rat skin sections post radiation and quantitative analysis of  $\gamma$ -H2AX-positive cells at different time points. (c, d) Representative immunofluorescence staining of TUNEL in rat skin sections post radiation and quantitative analysis of TUNEL-positive cells at different time points. (e, f) Representative immunofluorescence pictures of Ki67 in rat skin sections post radiation and quantitative analysis of Ki67-positive cells at different time points. The immunofluorescence staining positive cells were calculated using Image J software. Data are presented as mean  $\pm$  standard deviation,  $n=3$ , one-way analysis of variance with Bonferroni's *post hoc* comparison, compared with day 0; \* $p < 0.05$ , \*\* $p < 0.01$ .  $\gamma$ -H2AX Phosphorylated histone H2AX, DAPI 4',6-diamidino-2-phenylindole, TUNEL terminal deoxynucleotidyl transferase-mediated fluorescein-dUTP nick-end labeling

have characterized the pathological course and progression of radiation ulcers and indicated that the established radiation ulcer animal models can mimic the progression of radiation ulcers in patients, which will help with further investigation of the pathological mechanisms and therapeutic strategies for radiation ulcers.

#### Association of cellular senescence with the progression of radiation ulcers

To further explore the mechanism of radiation ulcer progression and the irreversible injury of skin from irradiated skin to

normal tissue, cellular senescence in irradiated skin samples was evaluated at different time points. We found an increase in SA- $\beta$ -gal activity in skin samples after irradiation, which is an accepted biomarker of cellular senescence. The number of senescent cells continuously increased as the radiation ulcer progressed and was maintained at a high level of senescence in the later stage of the radiation ulcer at day 60 (Figure 3a). We also detected cellular senescence in irradiated skin tissue by immunofluorescence staining of p16 and p21. The results showed accumulation of senescent cells in the irradiated tissue as the ulcer progressed, mainly distributed in the basal layer of the epidermis and dermis of the skin (Figure 3b, c

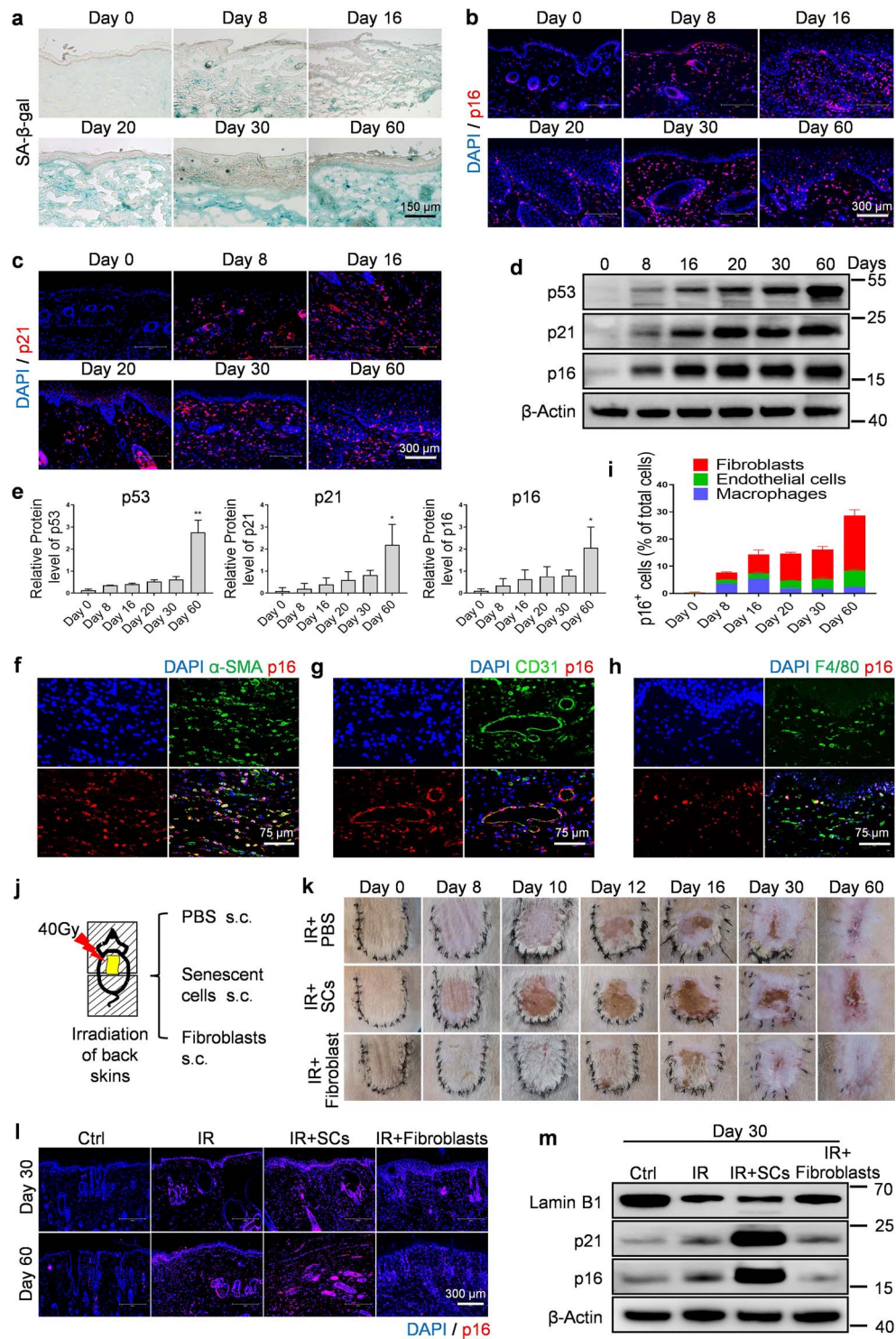


**Figure 3.** Characterization of cellular senescence in the progression of radiation ulcer rat models. (a) Representative SA- $\beta$ -gal staining pictures in irradiated rat skins. (b) Representative immunofluorescence pictures of p16 in skins after radiation. (c) Representative immunofluorescence pictures of p21 in irradiated skins. (d, e) Western blot analysis and quantification of p16, p21 and p53 in skin tissues after radiation. (f–h) Representative immunofluorescence pictures of p16 in irradiated skin sections;  $\alpha$ -SMA, CD31 and F4/80 were used to label the fibroblasts, endothelial cells and macrophages in skins, respectively. (i) Quantitative analysis of p16 positive cells in fibroblasts, endothelial cells and macrophages, respectively. (j) Schematic representation of back skin radiation ulcer models. (k) Representative images of back skins in different group rats. (l) Representative immunofluorescence pictures of p16 in skin sections at 30 or 60 days after 40 Gy radiation. (m) Western blot analysis of the expression levels of p16, p21 and lamin B1 in skin tissues at 30 days after irradiation. Data are presented as mean  $\pm$  standard deviation,  $n=3$ , one-way analysis of variance with Bonferroni's *post hoc* comparison, compared with day 0; \* $p < 0.05$ , \*\* $p < 0.01$ . *Ctrl* control, *IR* ionizing radiation,  $\alpha$ -SMA alpha-smooth muscle actin, *SCs* senescent cells, *Lamin B1* nuclear lamina protein lamin B1, *DAPI* 4',6-diamidino-2-phenylindole, *F4/80* mouse EGF-like module-containing mucin-like hormone receptor-like 1,  $\alpha$ -SMA  $\alpha$ -smooth muscle actin, *CD31* platelet endothelial cell adhesion molecule-1, SA- $\beta$ -gal senescence-associated  $\beta$ -galactosidase, *s.c.* subcutaneous injection

and Figure S1, see online supplementary material). Cellular senescence continued to increase even at 160 days post-irradiation (Figure S2, see online supplementary material). Similarly, western blotting detection also indicated increased expression of the senescence-related proteins p16, p21 and p53 in skin after irradiation (Figure 3d, e). To further study the cell type of senescence in radiation ulcers, we tested senescence in different cell types by staining with  $\alpha$ -SMA, CD31 and F4/80 to identify fibroblasts, vascular endothelial cells and macrophages, respectively, which are the most important cells for tissue repair in skin injury [18]. All of these cell type makers co-stained with p16, indicating that senescence occurred in all three cell types after radiation (Figure 3f, g, h). The co-stained cell statistical analysis indicated that senescent macrophages mainly appeared in the early stage of radiation injury, while senescent dermal fibroblasts and endothelial cells were persistently increased after irradiation (Figure 3i). Therefore, these results indicated that the accumulation of senescent cells is an important mechanism for the progression of radiation ulcers. To explore the specific function of senescent cells in the progression of radiation ulcers, we established senescent dermal fibroblasts by 8 Gy irradiation *in vitro* and then subcutaneously injected them into the irradiated back skin of rats (Figure 3j). We found that exogenous transplantation of senescent cells aggravated radiation ulcer progression and promoted radiation ulcer severity when compared with radiated ulcer models. Normal dermal fibroblasts were able to effectively delay the formation of radiation ulcers (Figure 3k). Immunofluorescence staining indicated that injection of senescent cells promoted radiation ulcers, with more p16-positive senescent cell accumulation in the irradiated skins when compared with irradiation alone (Figure 3l). Similarly, western blot also showed an increased level of cellular senescence in skin after the rats were injected with senescent cells (Figure 3m and Figure S3, see online supplementary material). Thus, these results indicate that cellular senescence is closely associated with the progression of radiation ulcers and that exogenous transplantation of senescent cells aggravates radiation ulcers.

#### Investigation of the underlying mechanisms associated with progression of radiation ulcers

To investigate the underlying mechanisms of senescent cells in promoting radiation ulcer progression, CM from senescent cells was collected to examine how senescent cells function in aggravating the progression of radiation ulcers. In this study, the CM from radiation-induced senescent cells (primary) was collected and cultured with normal fibroblasts for 10 days, and CM from secondary senescent cells was also collected and cultured with normal fibroblasts (tertiary), then all the CM-cultured cells phenotypes were detected (Figure 4a). Our results indicated that CM from primary and secondary cells could induce normal fibroblast senescence with the expression of SA- $\beta$ -gal and p16 (Figure 4b, c). qRT-PCR analysis showed that CM from primary senescent cells induced higher levels of senescent genes and the proinflammatory genes

IL-1 $\alpha$ , IL-1 $\beta$ , IL-6 and IL-10 than CM from secondary cells (Figure S4, primers are shown in Table S2, see online supplementary material). Therefore, the accumulation of senescent cells may induce paracrine senescence through complex secretions in radiation ulcers. To further investigate how senescent cells promote the progression of radiation ulcers, radiation-induced senescent cells (primary) and CM-induced senescent cells (secondary) were collected and subjected to RNA sequencing. We observed that 999 genes had significant differential expression levels with at least a 2-fold change ( $p < 0.05$ ) in primary senescent cells compared to normal cells, with 506 genes being upregulated and 493 genes being downregulated (Figure 4d, e). KEGG pathway enrichment analysis of the DEGs in primary senescent cells revealed that the upregulated genes were mainly enriched in PI3K-Akt signaling, pathways in cancer and cytokine-cytokine receptor interactions (Figure 4f). The main genes involved in the enriched pathways were Ccnd2, Cdkn1a, Cdkn1b, Cxcl2, Lamb3, Ccl11, Il33, Il34, Csf2, Csf2rb, Csf3, Cx3cl1, Cxcl13, Cxcl14 and Ano3, which are all active in senescent cells. For the secondary senescent cells, we observed that 1252 genes had significant differential expression when compared to normal cells, with 718 genes being upregulated and 534 genes being downregulated (Figure 4g, h). KEGG pathway enrichment analysis showed that the DEGs in the secondary senescent cells were enriched in the cell cycle, cytokine-cytokine receptor interactions and cellular senescence (Figure 4i). The main genes involved in the enriched pathways were Ccna2, Ccnb1, Cdk1, Cdkn2c, Ccl12, Cxcl14, Cxcl2, Gdf15, Il11, Il15, Il1a, Il1b, E2f1, E2f2 and Foxm1, which are all active in senescent cells and inflammatory cells. In addition, we performed enrichment analysis of the filtered upregulated genes between primary senescent cells and secondary senescent cells and found that 71 DEGs were upregulated in both groups of cells, as shown in the Venn diagram (Figure 4j). KEGG pathway analysis showed that these 71 DEGs were significantly enriched in cellular senescence, pathways in cancer and p53 signaling (Figure 4k), indicating that both cell lines have a senescent cell phenotype. Collectively, these findings suggested that CM from senescent cells could induce cellular senescence, but the DEGs and pathways associated with senescence were different from those in primary senescent cells.

#### uMSC-CM mitigates radiation ulcers by inhibiting cellular senescence

MSCs and their secretions (CM, extracellular vesicles and exosomes) have been regarded as promising options for difficult-to-treat wounds [19,20]. Here, uMSC-CM was used to determine whether MSC-CM could mitigate radiation ulcers. After eight intraperitoneal injections of 2 mg/kg uMSC-CM every other day in radiation ulcer rat models, our results indicated that uMSC-CM significantly alleviated radiation ulcer progression by reducing the pathological changes of exudation, crusting and ulceration after irradiation (Figure 5a). In addition, ELISA detection showed that the level of IL-1 $\alpha$  in the serum of rats treated with

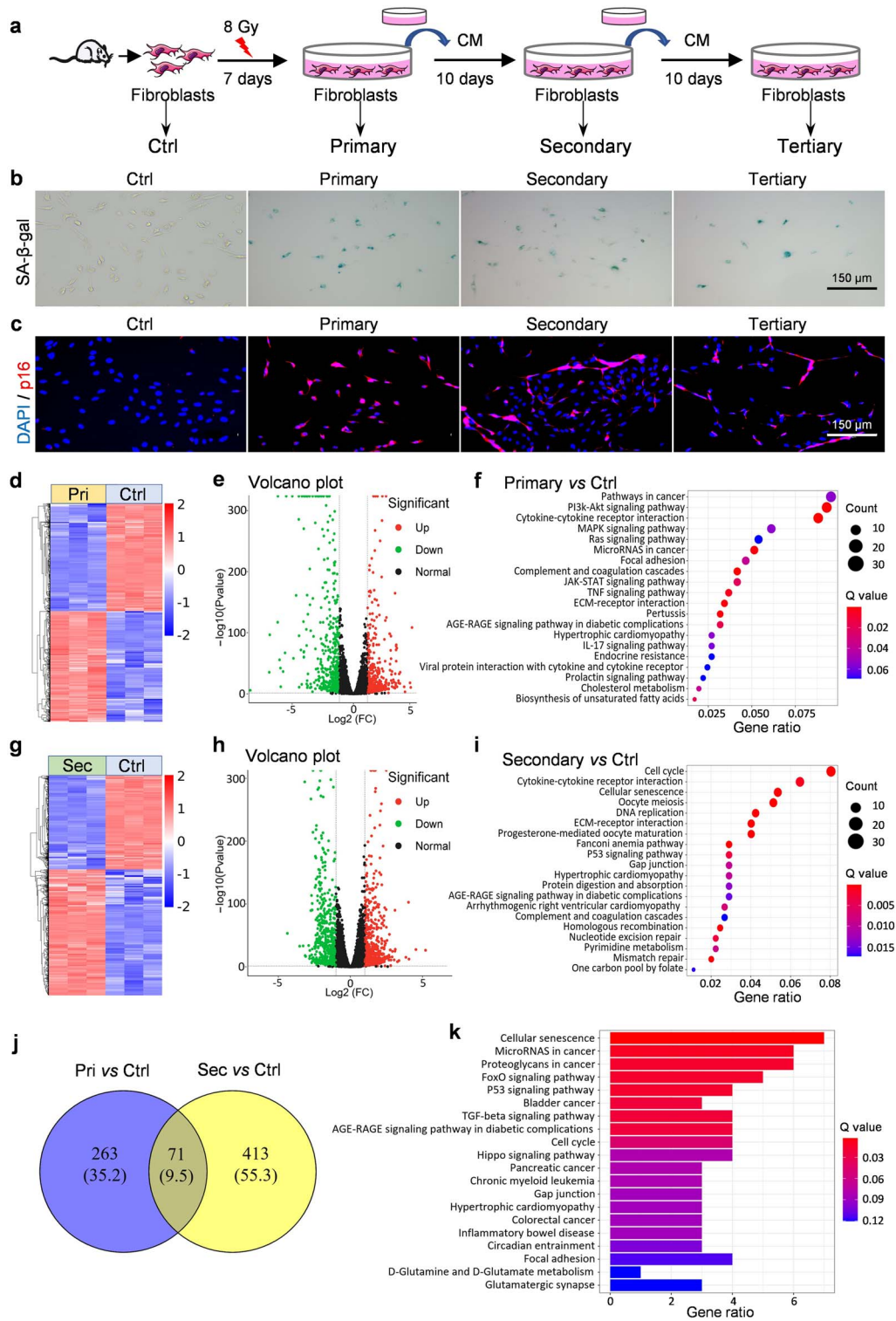


**Figure 4.** Analysis of the roles of senescent cells in the progression of radiation ulcers *in vitro*. (a) Schematic representing the serial transfer of senescence with CM. (b) SA-β-gal staining of cells cultured with different CM. (c) Representative immunofluorescence images of p16 in cells. (d) Heatmap plot of dysregulated mRNAs between normal cells and primary senescent cells. (e) Volcano plot of the differentially expressed mRNAs between normal cells and primary senescent cells. (f) KEGG pathway analysis of upregulated genes between normal cells and primary senescent cells. (g) Heatmap plot of dysregulated mRNAs between normal cells and secondary senescent cells. (h) Volcano plot of the differentially expressed mRNAs between normal cells and secondary senescent cells. (i) KEGG pathway analysis of upregulated genes between normal cells and secondary senescent cells. (j) Venn diagram of upregulated genes between primary senescent cells and secondary senescent cells. (k) KEGG pathway analysis of upregulated genes between primary senescent cells and secondary senescent cells. *Ctrl* control, *IR* ionizing radiation, *CM* conditioned medium, *Pri* primary, *Sec* secondary, *KEGG* Kyoto Encyclopedia of Genes and Genomes, *DAPI* 4',6-diamidino-2-phenylindole

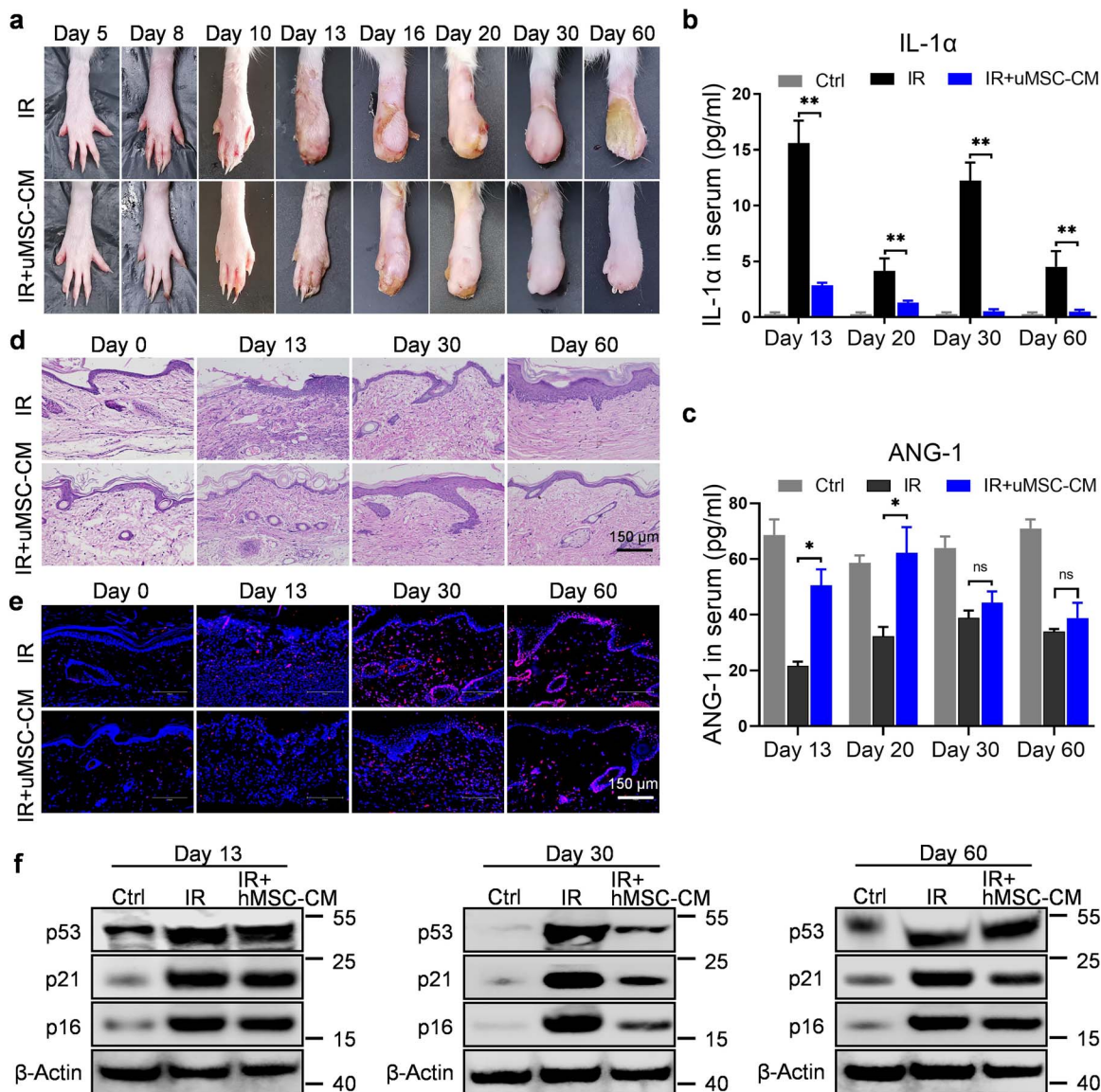


**Figure 5.** uMSC-CM inhibits the progression of radiation ulcer in rat models. (a) Representative images of hind limbs from irradiated rats and uMSC-CM treatment rats. (b) ELISA analysis the serum level of IL-1 $\alpha$  in different group rats. (c) ELISA analysis the serum level of ANG-1 in different group rats. (d) Histological analysis of skin tissues from irradiated rats and uMSC-CM treatment rats. (e) Representative immunofluorescence pictures of p16 in skin sections from irradiated rats and uMSC-CM treatment rats. (f) Western blot analysis of p16, p21 and p53 expression in different group rats. Data are presented as mean  $\pm$  SD,  $n=3$ , two-way analysis of variance with Bonferroni's *post hoc* comparison; \* $p < 0.05$ , \*\* $p < 0.01$ . Ctrl control, IR ionizing radiation, ns no significance, uMSC-CM conditioned medium derived from human umbilical cord mesenchymal stem cells, IL-1 $\alpha$  interleukin-1 $\alpha$ , ANG-1 angiopoietin-1

uMSC-CM was significantly decreased compared with that in the control group (Figure 5b). Additionally, the level of ANG-1 was rescued by treatment with uMSC-CM (Figure 5c). Histopathological analysis showed that uMSC-CM treatment significantly reduced inflammation after irradiation and protected against radiation-induced hair follicle, gland and capillary damage in the late stage (Figure 5d). Meanwhile, immunofluorescence staining and western blotting showed that uMSC-CM treatment significantly decreased the expression of the senescence-related genes p16, p21 and p53 compared with irradiated skins (Figure 5e, f). Thus, the uMSC-CM obviously mitigated the progression of radiation ulcers by reducing cellular senescence and senescent

secretions *in vivo*. For the *in vitro* assay, 500 ng/ml uMSC-CM was used and significantly alleviated radiation-induced DNA damage by reducing  $\gamma$ -H2AX expression in irradiated dermal fibroblasts (Figure 6a, b). In addition, uMSC-CM treatment was also shown to inhibit senescence by decreasing SA- $\beta$ -gal activity in irradiated dermal fibroblasts (Figure 6c, d). We found that the expression of senescence genes and proinflammatory genes was decreased after irradiated dermal fibroblasts were treated with uMSC-CM *in vitro* by qRT-PCR (Figure 6e, f). Western-blot analysis indicated that uMSC-CM treatment decreased the expression levels of senescence markers in irradiated dermal fibroblasts (Figure 6g). Taken together, these results indicated that uMSC-CM effectively

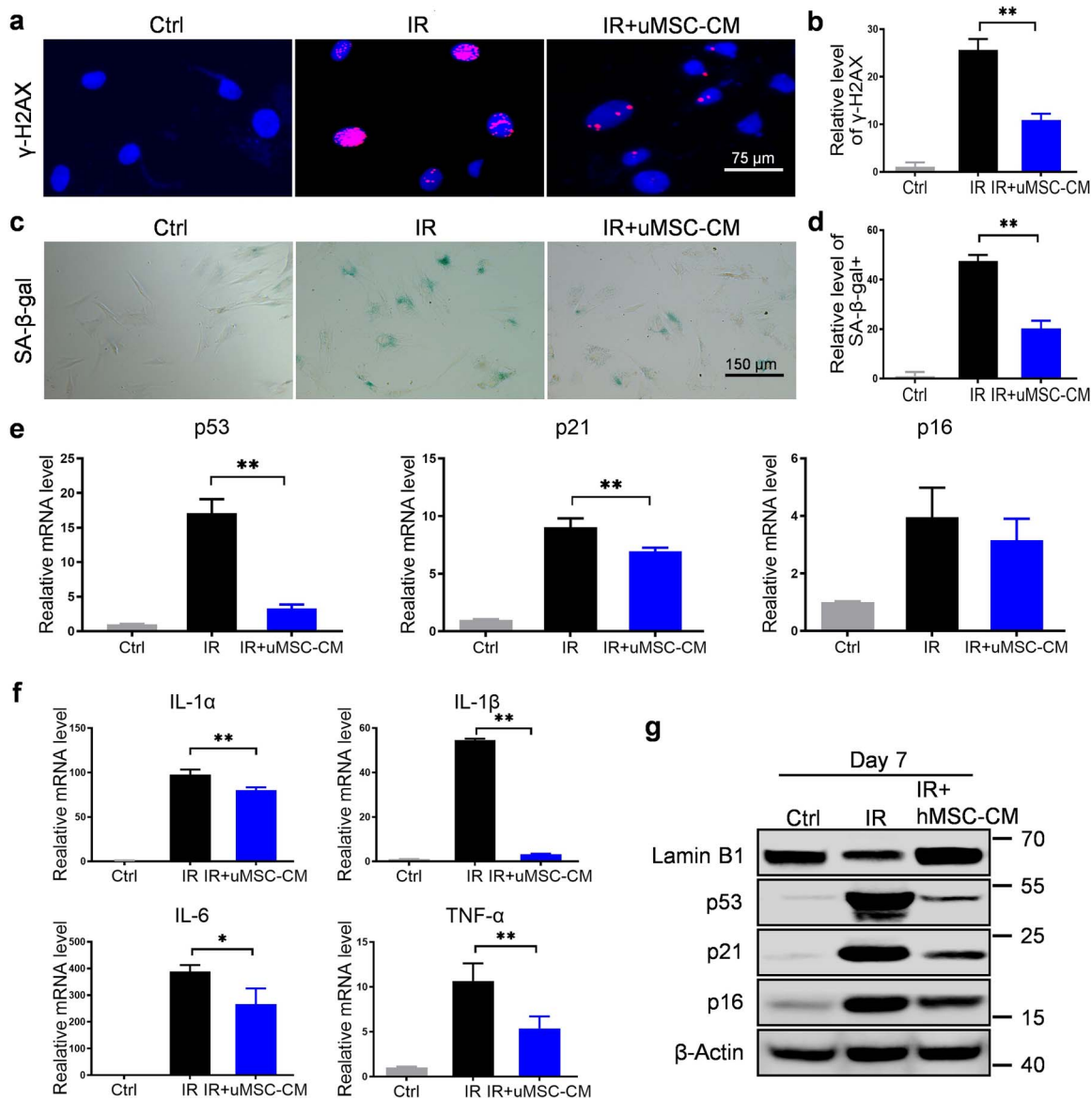


**Figure 6.** uMSC-CM treatment decreases radiation-induced cellular senescence *in vitro*. (a, b) Representative immunofluorescence pictures of  $\gamma$ -H2AX in different treated fibroblasts and quantitative analysis of  $\gamma$ -H2AX-positive cells. (c, d) Representative images of SA- $\beta$ -gal staining in different treated fibroblasts and quantitative analysis of SA- $\beta$ -gal-positive cells. (e) Real-time qPCR detection of senescence-related genes p16, p21 and p53 expression in normal, irradiated and uMSC-CM (500 ng/ml)-treated fibroblasts. (f) Real-time qPCR detection of proinflammatory genes IL-1 $\alpha$ , IL-1 $\beta$ , IL-6 and TNF- $\alpha$  expression in normal, irradiated and uMSC-CM treated fibroblasts. (g) Western blot analysis of p16, p21, p53 and lamin B1 expression in normal, irradiated and uMSC-CM-treated fibroblasts. Data are presented as mean  $\pm$  SD,  $n=3$ , one-way analysis of variance with Bonferroni's *post hoc* comparison; \* $p < 0.05$ , \*\* $p < 0.01$ . Ctrl control, IR ionizing radiation, uMSC-CM conditioned medium derived from human umbilical cord mesenchymal stem cells, IL-1 $\beta$  interleukin-1 $\beta$ , TNF- $\alpha$  tumor necrosis factor  $\alpha$ ,  $\gamma$ -H2AX phosphorylated histone H2AX, SA $\beta$ -gal senescence-associated  $\beta$ -galactosidase

mitigated the progression of radiation ulcers by inhibiting cellular senescence, suggesting that the use of uMSC-CM is a potential effective strategy for the treatment of radiation ulcers.

## Discussion

As radioactive materials and technology have been widely used in different fields, including industry and medicine, they have significantly increased the probability of uncontrolled

radiation exposure to human beings [21]. Radiation-induced skin injury is the most common accidental exposure to radiation since the skin is the largest organ of the body and is a radiosensitive organ system [22,23]. It has been reported that >95% of cancer patients who receive radiotherapy develop some form of radiation dermatitis [24]. Radiation-induced skin injury not only limits radiotherapy in clinical practice but also severely hampers the quality of life and survival of patients [25]. Moreover, high-dose or multiple irradiations can induce radiation ulcers, which are the most

distressed and difficult-to-heal skin injuries, accompanied by progressive ulceration, delayed healing and irreversible functional loss of skin [26]. Previous studies have suggested that ionizing radiation-induced DNA damage and ROS production are the main causes of radiation-induced injury [6,7]. Radiation-induced cell death and oxidative stress injury do not fully characterize the pathological mechanism and progression of radiation ulcers. Therefore, more research efforts are needed to uncover the underlying mechanisms responsible for the progression of radiation ulcers, and novel therapeutic strategies are required to manage the risk of radiation ulcers.

Recently, increasing evidence has indicated that cellular senescence plays an important role in chronic wounds, including radiation ulcers, pressure ulcers and diabetic foot ulcers [12]. Previous studies have reported that the accumulation of senescent cells is involved in radiation ulcers, and preventing cellular senescence or removing senescent cells holds promise in mitigating radiation ulcers [13]. However, the characteristics of senescence in the progression of radiation ulcers and the underlying roles of senescent cells in their promotion remains to be further clarified. In this study, radiation ulcer rat models were established and skin injury was continuously evaluated for >260 days. Our results indicated that a single high dose of irradiation induced sustained progressive ulcers, but with remission of the ulceration phenotype ~20–30 days after radiation (Figure 1). Considering the continuous accumulation of senescent cells in irradiated skin tissue (Figure 2), we believe that senescent cells may play a crucial role in promoting the secondary progression of radiation ulcers after temporary relief and may even cause damage to nonirradiated skin. In addition, we observed that the expression of p16 was stably upregulated over time, but the expression of p21 was only significantly upregulated after 30 days. p16 and p21 are both considered biomarkers of cellular senescence. p16 is a negative cell cycle regulator that inhibits the cyclin-dependent kinases CDK4 and CDK6 and remains highly expressed during cellular senescence progression [27], while p21 is downstream of phosphorylated p53, which inhibits the cyclin-CDK complex by binding to CDK2 [28]. The latest research has reported that in addition to the classical role of cell cycle arrest, p21 may act as a monitoring mechanism for maintaining homeostasis after stress or injury [29], which may be the reason why the level of p16 was increased earlier than that of p21. At the same time, we found that different cell types exhibiting senescence appeared in different proportions in the progression of radiation ulcers. Senescent macrophages mainly appeared in the first stage of ulcers, while senescent fibroblasts and endothelial cells played important roles in the secondary progression of radiation ulcers (Figure 3i). Moreover, both primary senescent cells and secondary senescent cells were demonstrated to promote normal cell senescence through cell secretions in radiation ulcers. This may be an important mechanism in the progression of radiation ulcers, but the genes and pathways associated with senescence in these senescent cells were

different, as detected by RNA sequencing (Figure 4). Further research efforts are needed to identify the key secretions and specific cytokines responsible for promoting radiation ulcer progression and severity. Thus, our results have revealed the pivotal roles of senescent cells in the progression of radiation ulcers and that senescence secretions might play important roles in inducing cellular senescence and radiation ulcer progression.

MSCs, identified as multipotent stromal cells with self-renewal potential and multilineage differentiation capacity, have been regarded as a promising therapeutic option for many injured tissues or chronic wounds that lack effective treatments [30–32]. MSCs can usually be derived from several sources, including the umbilical cord, bone marrow, skin dermis and fat tissue, making them an ideal candidate cell type for tissue repair and regeneration [33,34]. Many previous studies have reported that the transplantation of MSCs could effectively facilitate the healing of chronic wounds and radiation wounds [35–37]. Meanwhile, subcutaneous injection of dermal fibroblasts was also found to mitigate the progression of radiation ulcers in rat models in this study (Figure 3k). Generally, the mechanisms of MSC-based wound therapy are postulated to be direct differentiation of MSCs into skin cells and the secretion of cytokines, growth factors, extracellular vesicles and exosomes by MSCs [38,39]. Considering the inefficient engraftment of MSCs at the site of wound injury and the risk of malignant transformation [40,41], recent studies have widely explored the therapeutic potential of MSC secretions in treating difficult-to-treat wounds [42,43]. In this study, standardized prepared uMSC-CM was intraperitoneally injected into radiation ulcer rat models at a dose of 2 mg/kg. Our results indicated that uMSC-CM significantly mitigated the progression of radiation ulcers by reducing the pathological changes of exudation, crusting and ulceration in irradiated skin. Moreover, uMSC-CM treatment alleviated radiation ulcers by inhibiting cellular senescence *in vivo* and *in vitro*, which further demonstrated the critical roles of senescent cells in the progression of radiation ulcers and suggested senescent cells as a practically effective target for radiation ulcer therapy.

## Conclusions

In this study, we characterized the vital roles of senescent cells in the progression of radiation ulcers by successfully establishing a series of radiation ulcer models. In addition, our results indicated that uMSC-CM could significantly alleviate radiation ulcers by inhibiting cellular senescence, which further demonstrated the critical roles of senescent cells in the progression of radiation ulcers and suggested that MSC-derived CM is a potential effective strategy for the treatment of radiation ulcers. Moreover, radiation-induced senescent cells are thought to facilitate senescence and promote the progression of radiation ulcers through complex senescent cell secretions, but the key regulators and specific mechanisms remain to be further detected.

## Abbreviations

ANG-1: Angiopoietin-1; ANOVA: Analysis of variance; CD31: Platelet endothelial cell adhesion molecule-1; CDK: Cyclin-dependent kinase; CM: Conditioned medium; DAPI: 4',6-Diamidino-2-phenylindole; DEGs: Differentially expressed genes; ELISA: Enzyme-linked immunosorbent assay; F4/80: Mouse EGF-like module-containing mucin-like hormone receptor-like 1; H&E: Hematoxylin–eosin;  $\gamma$ -H2AX: Phosphorylated histone H2AX; IL-1 $\beta$ : Interleukin-1 $\beta$ ; KEGG: Kyoto Encyclopedia of Genes and Genomes; SA- $\beta$ -gal: Senescence-associated  $\beta$ -galactosidase; Lamin B1: Nuclear lamina protein LMNB1; ROS: Reactive oxygen species; SD: Sprague–Dawley;  $\alpha$ -SMA:  $\alpha$ -Smooth muscle actin; uMSC-CM: Human umbilical cord mesenchymal stem cells-derived conditioned medium; TUNEL: Terminal deoxynucleotidyl transferase-mediated fluorescein-dUTP nick-end labeling; NRF2: Nuclear factor erythroid 2-related factor 2; AMPK: Adenosine monophosphate-activated protein kinase; PBS: Phosphate buffered saline; BCA: Bicinchoninic acid; DMEM: Dulbecco's modified eagle medium;  $\alpha$ -MEM: Minimum essential medium-alpha; PVDF: Polyvinylidene fluoride; qRT-PCR: Quantitative real time polymerase chain reaction; PI3K/AKT: Phosphatidylinositol 3-kinase/protein kinase B.

## Supplementary data

Supplementary data is available at *Burns & Trauma* Journal online.

## Funding

This work was supported by the Key Program of the National Natural Science Foundation of China (82030056), the Intramural Research Project Grants (2021-JCJQ-ZD-077-11, AWS17J007 and 2018-JCJQ-ZQ-001) and Post-doctoral Innovative Talent Support Program in Chongqing (CQBX2021010).

## Data availability

Data and materials related to this work are available from the corresponding author upon request.

## Authors' contributions

WC, Yang Wang and CS designed the research studies. WC, Yang Wang, JZ, YC, WY, CZ and LW conducted experiments. WC, JZ and LW acquired data. WC, ZY and Yu Wang analyzed data. WC, Yang Wang and CS wrote the manuscript. All authors read and approved the final manuscript.

## Ethics approval and consent to participate

Protocols for experiments involving animals were approved by the Animal Care and Use Committee of the Army Medical University.

## Conflicts of interests

None declared.

## References

- Wei J, Meng L, Hou X, Qu C, Wang B, Xin Y, *et al*. Radiation-induced skin reactions: mechanism and treatment. *Cancer Manag Res*. 2019;11:167–77. <https://doi.org/10.2147/CMAR.S188655>.
- Frazier TH, Richardson JB, Fabre VC, Callen JP. Fluoroscopy-induced chronic radiation skin injury: a disease perhaps often overlooked. *Arch Dermatol*. 2007;143:637–40. <https://doi.org/10.1001/archderm.143.5.637>.
- Ma X, Jin Z, Li G, Yang W. Classification of chronic radiation-induced ulcers in the chest wall after surgery in breast cancers. *Radiat Oncol*. 2017;12:135. <https://doi.org/10.1186/s13014-017-0876-y>.
- Hampton AL, Hish GA, Aslam MN, Rothman ED, Bergin IL, Patterson KA, *et al*. Progression of ulcerative dermatitis lesions in C57BL/6Crl mice and the development of a scoring system for dermatitis lesions. *J Am Assoc Lab Anim Sci*. 2012;51: 586–93.
- Hymes SR, Strom EA, Fife C. Radiation dermatitis: clinical presentation, pathophysiology, and treatment 2006. *J Am Acad Dermatol*. 2006;54:28–46. <https://doi.org/10.1016/j.jaad.2005.08.054>.
- Ahamed J, Laurence J. Role of platelet-derived transforming growth factor-beta1 and reactive oxygen species in radiation-induced organ fibrosis. *Antioxid Redox Signal*. 2017;27:977–88. <https://doi.org/10.1089/ars.2017.7064>.
- Schutz CS, Stope MB, Bekeschus S. H2A.X phosphorylation in oxidative stress and risk assessment in plasma medicine. *Oxidative Med Cell Longev*. 2021;2021:2060986. <https://doi.org/10.1155/2021/2060986>.
- Khosla S, Farr JN, Monroe DG. Cellular senescence and the skeleton: pathophysiology and therapeutic implications. *J Clin Invest*. 2022;132:3. <https://doi.org/10.1172/JCI154888>.
- Al-Jumayli M, Brown SL, Chetty IJ, Extermann M, Movsas B. The biological process of aging and the impact of ionizing radiation. *Semin Radiat Oncol*. 2022;32:172–8. <https://doi.org/10.1016/j.semradonc.2021.11.011>.
- Park H, Kim CH, Jeong JH, Park M, Kim KS. GDF15 contributes to radiation-induced senescence through the ROS-mediated p16 pathway in human endothelial cells. *Oncotarget*. 2016;7:9634–44. <https://doi.org/10.18632/oncotarget.7457>.
- Khan MGM, Wang Y. Advances in the current understanding of how low-dose radiation affects the cell cycle. *Cell*. 2022;11:3. <https://doi.org/10.3390/cells11030356>.
- Wang ZW, Shi CM. Cellular senescence is a promising target for chronic wounds: a comprehensive review. *Burns & Trauma*. 2020;8. <https://doi.org/doi ARTN tkaa02110.1093/burnst/kaa021>.
- Wang Z, Chen Z, Jiang Z, Luo P, Liu L, Huang Y, *et al*. Cordycepin prevents radiation ulcer by inhibiting cell senescence via NRF2 and AMPK in rodents. *Nat Commun*. 2019;10:2538. <https://doi.org/10.1038/s41467-019-10386-8>.
- Wang H, Wang Z, Huang Y, Zhou Y, Sheng X, Jiang Q, *et al*. Senolytics (DQ) mitigates radiation ulcers by removing senescent cells. *Front Oncol*. 2019;9:1576. <https://doi.org/10.3389/fonc.2019.01576>.

15. Kumar S, Kolozsvary A, Kohl R, Lu M, Brown S, Kim JH. Radiation-induced skin injury in the animal model of scleroderma: implications for post-radiotherapy fibrosis. *Radiat Oncol*. 2008;3:40. <https://doi.org/10.1186/1748-717X-3-40>.
16. Gneccchi M, He H, Noiseux N, Liang OD, Zhang L, Morello F, et al. Evidence supporting paracrine hypothesis for Akt-modified mesenchymal stem cell-mediated cardiac protection and functional improvement. *FASEB J*. 2006;20:661–9. <https://doi.org/10.1096/fj.05-5211com>.
17. Li B, Dewey CN. RSEM: accurate transcript quantification from RNA-Seq data with or without a reference genome. *BMC Bioinformatics*. 2011;12:323. <https://doi.org/10.1186/1471-2105-12-323>.
18. Rong X, Li J, Yang Y, Shi L, Jiang T. Human fetal skin-derived stem cell secretome enhances radiation-induced skin injury therapeutic effects by promoting angiogenesis. *Stem Cell Res Ther*. 2019;10:383. <https://doi.org/10.1186/s13287-019-1456-x>.
19. Marofi F, Alexandrova KI, Margiana R, Bahramali M, Sukatan W, Abdelbasset WK, et al. MSCs and their exosomes: a rapidly evolving approach in the context of cutaneous wounds therapy. *Stem Cell Res Ther*. 2021;12:597. <https://doi.org/10.1186/s13287-021-02662-6>.
20. Varderdidou-Minasian S, Lorenowicz MJ. Mesenchymal stromal/stem cell-derived extracellular vesicles in tissue repair: challenges and opportunities. *Theranostics*. 2020;10:5979–97. <https://doi.org/10.7150/thno.40122>.
21. Buchberger B, Scholl K, Krabbe L, Spiller L, Lux B. Radiation exposure by medical X-ray applications. *Ger. Med Sci*. 2022;20:Doc06. <https://doi.org/10.3205/000308>.
22. Lee YI, Choi S, Roh WS, Lee JH, Kim TG. Cellular senescence and Inflammaging in the skin microenvironment. *Int J Mol Sci*. 2021;22:8. <https://doi.org/10.3390/ijms22083849>.
23. Wai KM, Krstic D, Nikezic D, Lin TH, Yu PKN. External Cesium-137 doses to humans from soil influenced by the Fukushima and Chernobyl nuclear power plants accidents: a comparative study. *Sci Rep*. 2020;10:7902. <https://doi.org/10.1038/s41598-020-64812-9>.
24. Spalek M. Chronic radiation-induced dermatitis: challenges and solutions. *Clin Cosmet Investig Dermatol*. 2016;9:473–82. <https://doi.org/10.2147/CCID.S94320>.
25. Nuta O, Somaiah N, Boyle S, Chua ML, Gothard L, Yarnold J, et al. Correlation between the radiation responses of fibroblasts cultured from individual patients and the risk of late reaction after breast radiotherapy. *Cancer Lett*. 2016;374:324–30. <https://doi.org/10.1016/j.canlet.2016.02.036>.
26. Bennardo L, Passante M, Cameli N, Cristaudo A, Patrucco C, Nistico SP, et al. Skin manifestations after ionizing radiation exposure: a systematic review. *Bioengineering (Basel)*. 2021;8:11. <https://doi.org/10.3390/bioengineering8110153>.
27. Sherr CJ, Beach D, Shapiro GI. Targeting CDK4 and CDK6: from discovery to therapy. *Cancer Discov*. 2016;6:353–67. <https://doi.org/10.1158/2159-8290.CD-15-0894>.
28. Engeland K. Cell cycle regulation: p53-p21-RB signaling. *Cell Death Differ*. 2022;29:946–60. <https://doi.org/10.1038/s41418-022-00988-z>.
29. Sturmlechner I, Zhang C, Sine CC, van Deursen EJ, Jeganathan KB, Hamada N, et al. p21 produces a bioactive secretome that places stressed cells under immunosurveillance. *Science*. 2021;374:eabb3420. <https://doi.org/10.1126/science.abb3420>.
30. Ren Y, Aierken A, Zhao L, Lin Z, Jiang J, Li B, et al. hUC-MSCs lyophilized powder loaded polysaccharide ulvan driven functional hydrogel for chronic diabetic wound healing. *Carbohydr Polym*. 2022;288:119404. <https://doi.org/10.1016/j.carbpol.2022.119404>.
31. Las Heras K, Royo F, Garcia-Vallicrosa C, Igartua M, Santos-Vizcaino E, Falcon-Perez JM, et al. Extracellular vesicles from hair follicle-derived mesenchymal stromal cells: isolation, characterization and therapeutic potential for chronic wound healing. *Stem Cell Res Ther*. 2022;13:147. <https://doi.org/10.1186/s13287-022-02824-0>.
32. Huang YZ, Gou M, Da LC, Zhang WQ, Xie HQ. Mesenchymal stem cells for chronic wound healing: current status of preclinical and clinical studies. *Tissue Eng Part B Rev*. 2020;26:555–70. <https://doi.org/10.1089/ten.TEB.2019.0351>.
33. Vishnubalaji R, Al-Nbaheen M, Kadalmani B, Aldahmash A, Ramesh T. Skin-derived multipotent stromal cells—an archival for mesenchymal stem cells. *Cell Tissue Res*. 2012;350:1–12. <https://doi.org/10.1007/s00441-012-1471-z>.
34. Shi Y, Hu G, Su J, Li W, Chen Q, Shou P, et al. Mesenchymal stem cells: a new strategy for immunosuppression and tissue repair. *Cell Res*. 2010;20:510–8. <https://doi.org/10.1038/cr.2010.44>.
35. Li X, Wang Y, Shi L, Li B, Li J, Wei Z, et al. Magnetic targeting enhances the cutaneous wound healing effects of human mesenchymal stem cell-derived iron oxide exosomes. *J Nanobiotechnology*. 2020;18:113. <https://doi.org/10.1186/s12951-020-00670-x>.
36. Xue J, Sun N, Liu Y. Self-assembled Nano-peptide hydrogels with human umbilical cord mesenchymal stem cell spheroids accelerate diabetic skin wound healing by inhibiting inflammation and promoting angiogenesis. *Int J Nanomedicine*. 2022;17:2459–74. <https://doi.org/10.2147/IJN.S363777>.
37. Huang SP, Huang CH, Shyu JF, Lee HS, Chen SG, Chan JY, et al. Promotion of wound healing using adipose-derived stem cells in radiation ulcer of a rat model. *J Biomed Sci*. 2013;20:51. <https://doi.org/10.1186/1423-0127-20-51>.
38. Liu Y, Zhang Z, Wang B, Dong Y, Zhao C, Zhao Y, et al. Inflammation-stimulated MSC-derived small extracellular vesicle miR-27b-3p regulates macrophages by targeting CSF-1 to promote temporomandibular joint condylar regeneration. *Small*. 2022;18:e2107354. <https://doi.org/10.1002/sml.202107354>.
39. Ardalan M, Chodari L, Zununi Vahed S, Hosseiniyan Khatibi SM, Eftekhari A, Davaran S, et al. Stem cell-derived biofactors fight against coronavirus infection. *World J Stem Cells*. 2021;13:1813–25. <https://doi.org/10.4252/wjsc.v13.i12.1813>.
40. Sarkar D, Spencer JA, Phillips JA, Zhao W, Schafer S, Spelke DP, et al. Engineered cell homing. *Blood*. 2011;118:e184–91. <https://doi.org/10.1182/blood-2010-10-311464>.
41. Sun J, Huang J, Bao G, Zheng H, Wang C, Wei J, et al. MRI detection of the malignant transformation of stem cells through reporter gene expression driven by a tumor-specific promoter. *Stem Cell Res Ther*. 2021;12:284. <https://doi.org/10.1186/s13287-021-02359-w>.
42. Jiang D, Scharffetter-Kochanek K. Mesenchymal stem cells adaptively respond to environmental cues thereby improving granulation tissue formation and wound healing. *Front Cell Dev Biol*. 2020;8:697. <https://doi.org/10.3389/fcell.2020.00697>.
43. Geng X, Qi Y, Liu X, Shi Y, Li H, Zhao L. A multifunctional antibacterial and self-healing hydrogel laden with bone marrow mesenchymal stem cell-derived exosomes for accelerating diabetic wound healing. *Mater Sci Eng C Mater Biol Appl*. 2021;112613. <https://doi.org/10.1016/j.msec.2021.112613>.